Toughening of phase-homogenized mixtures of nylon-6 and poly(*m*-xylene adipamide) with a functionalized block copolymer

Y. Takeda*, H. Keskkula and D. R. Paul†
Department of Chemical Engineering and Center for Polymer Research, The University of Texas at Austin, Austin, TX 78712, USA
(Received 15 June 1991; revised 26 August 1991; accepted 25 September 1991)

Mixtures of nylon-6 and poly(*m*-xylene adipamide) (MXD6) undergo sufficient interchange reactions when melt blended at 290°C to give a homogeneous melt phase and a material with a single T_g. However, the extent of reaction is sufficiently low that the product retains a high level of ability to crystallize. These phase-homogenized mixtures become supertough when blended with a maleic anhydride (MA) grafted elastomeric styrene–(ethylene/butene)–styrene (SEBS) triblock copolymer, i.e. SEBS-*g*-MA. Pure nylon-6, pure MXD6, or mixtures of the two prepared under low-temperature extrusion conditions (260°C) that do not lead to phase homogenization are not similarly supertoughened by blending with SEBS-*g*-MA. The reasons appear to relate to differences in elastomer particle morphology and inherent ductility for the various matrices. SEBS-*g*-MA blends with nylon-6 are not supertough because the rubber particles are too small. Addition of MXD6 causes the particles to become larger and of optimum size for toughening, but it is postulated that MXD6 is difficult to toughen because of low inherent ductility. The polyamide mixtures that were not phase homogenized are also inherently incompatible. The differences in rubber particle geometry are explained in terms of the functionality of the two polyamides towards reactions with anhydride groups.

(Keywords: blends; polyamides; interchange reactions; toughening; phase homogeneity; copolymers)

INTRODUCTION

In a previous paper[1] we described how blends of nylon-6 and the partially aromatic polyamide poly(*m*-xylene adipamide) (MXD6) can be melt-phase-homogenized by interchange reactions during high-temperature extrusion. As few as five reactions per chain appear to be sufficient to lead to a homogeneous melt[2] since evidently the nylon-6–MXD6 interaction is only weakly repulsive[2]. Because of its blocky nature, the resulting copolymer of nylon-6 and MXD6 formed during melt extrusion retains a remarkably high ability to crystallize. This paper focuses on the mechanical properties of the nylon-6/MXD6 materials and of their blends with a maleated elastomer that is useful for rubber toughening of polyamides[3–6]. The particular elastomer used is a sytrene–butadiene–styrene triblock copolymer whose mid-block has been hydrogenated (to resemble an ethylene/butene random copolymer) and then grafted with maleic anhydride (MA). Thus, the base elastomer is designated as SEBS and the maleated version as SEBS-*g*-MA.

Rubber toughening of polyamides with maleated elastomers has been described extensively in the literature[3–23]. It is well known that nylon-6 and nylon-6,6 only achieve supertoughness when the rubber is very finely dispersed, i.e. rubber particles less than 1 μm in diameter. Wu[7,8] has argued that interparticle distance rather than particle diameter *per se* is the more fundamental criterion for achieving toughness. Recent work[3,4,6] has revealed some striking differences between nylon-6 and nylon-6,6 in terms of morphology generation and toughening response. Nylon-6 does not become supertough when blended with the commercially available SEBS-*g*-MA, but dilution of the SEBS-*g*-MA with appropriate amounts of non-reactive SEBS leads to supertough nylon-6 compositions. On the other hand, nylon-6,6 becomes supertough when blended with SEBS-*g*-MA alone, and addition of SEBS only diminishes toughness. These results have been explained in terms of morphological differences. Melt blending of SEBS-*g*-MA alone with nylon-6 produces extremely fine rubber particles ($\sim$0.05 μm) that are too small for effective toughening, and dilution of the rubber phase with the non-reactive SEBS increases particle size to within the optimal range[3,4]. Of course, blending with SEBS alone yields particles that are too large ($\sim$5 μm) (and most likely lack adequate adhesion to the polyamide matrix) for toughening. Melt blending of SEBS-*g*-MA with nylon-6,6 results in particles that are already in the optimal range for toughening, i.e. much larger than for SEBS-*g*-MA in nylon-6 but smaller than those for SEBS in either nylon-6 or nylon-6,6. We proposed[3,4] that the differences in morphology of blends of SEBS-*g*-MA with nylon-6 and nylon-6,6 stem from fundamental chemical differences between the two polyamides. Nylon-6 is always monofunctional in terms of its reactions with an

*Permanent address: Mitsubishi Gas Chemical Co., 22 Wadai Tsukuba-shi, 300-42, Japan
†To whom correspondence should be addressed

0032-3861/92/163394-14

anhydride-containing phase so that only simple grafting, i.e. one attachment per polyamide chain, can occur. Nylon-6,6 can be difunctional in its reactions with anhydrides, i.e. two attachments per polyamide chain are possible. Their functionality is the same whether the polyamide reaction with anhydrides involves amine ends or amide linkages[4,17,19,21]. Multiple chain connections can act to prevent particle break-up or separation, encourage coalescence and provide a clear mechanism for occlusion of matrix material into the rubber particles. For any of these mechanisms, coarser reactive rubber particles are then expected in difunctional polyamides compared to monofunctional ones.

In the present case, MXD6 is a difunctional polyamide like nylon-6,6 and this appears to be an important issue in the results described here. On the other hand, MXD6 is evidently not inherently very ductile, so unlike nylon-6,6 it is not readily toughened by directly blending with SEBS-*g*-MA.

MATERIALS AND PROCEDURES

The nylon-6 was obtained from Allied-Signal Inc. while the MXD6 nylon made from *m*-xylene diamine and adipic acid was obtained from Mitsubishi Gas Chemical Co. Two styrene–(ethylene/butene)–styrene triblock copolymers were obtained from Shell Chemical Co. One contained 1.84 wt% grafted maleic anhydride, SEBS-*g*-MA, while the other was not functionalized, SEBS. Further details about these materials are given in *Table 1*.

Nylon-6/MXD6 blends of various compositions were phase-homogenized by melt mixing at 290°C by a single pass through a Killion single-screw extruder ($L/D = 30$, 2.54 cm diameter). This homogenization is caused by interchange reactions as described previously[1]. As controls, blends of nylon-6 and MXD6 were extruded once at 260°C – a condition where the extent of interchange reaction is not sufficient to lead to phase homogenization. For the purpose of toughening, the nylon mixtures were extrusion-compounded with the elastomeric triblock copolymer by a single pass through the Killion extruder at 260°C. Mixtures of SEBS-*g*-MA and SEBS were prepared by extrusion at 200°C before blending with nylon. The extruded materials were injection-moulded into standard tensile (ASTM D638 type I) and Izod (ASTM D256) bars (0.318 cm thick) using an Arburg All-rounder screw injection-moulding machine. Before extrusion and injection moulding, all samples were dried in a vacuum oven at 100°C for at least 12 h.

Some specimens were tested directly, dry as-moulded, while others were annealed at 100°C for 12 h in a vacuum oven before measuring mechanical properties. This annealing increased crystallinity and thus changed some properties; however, it also served to reduce the scatter in the mechanical property data relative to unannealed specimens.

A Brabender torque rheometer was used for melt rheological characterization of the various components and to demonstrate reaction grafting. Values of torque quoted in the following were measured at 260°C and 60 rev min^{-1} after fluxing for 10 min.

Tensile properties were measured at room temperature using an Instron at a crosshead speed of 5.08 cm min^{-1}. Izod impact strengths were determined using bars 0.318 cm thick with a TMI tester. All measurements were made at room temperature except where indicated otherwise. A Dynatup impact testing system was used to examine the effect of impact speed on toughness at room temperature. The initial height of the tup (mass = 9.5 kg) was adjusted to achieve impact velocities between 0.5 to 3.0 m s^{-1} as measured by the velocity sensor.

Dynamic mechanical testing was performed using a Polymer Laboratories Dynamic Mechanical Thermal Analyzer, at a frequency of 3 Hz and a heating rate of 2°C min^{-1}. Annealed Izod bars were used for the d.m.t.a. measurements.

Heats of fusion, ΔH, were measured using a Perkin–Elmer differential scanning calorimeter (DSC-7) at a scan rate of 20°C min^{-1}. Each ΔH was determined during the first scan of a specimen excised from an Izod bar and was defined as the area integrated from 155 to 245°C. The melting peaks of nylon-6 and MXD6 overlap and cannot be resolved, so the ΔH obtained is the sum of the individual heats of fusion.

Blend morphology was examined by an NEC transmission electron microscope (JEM-2000FX). Samples were microtomed from Izod bars perpendicular to the flow direction and stained with RuO_4.

Table 1 Materials used

Designation	Material (commercial designation)	Molecular weight	Relative melt viscosity[a]	Source
Nylon-6	Poly(ε-caprolactam) (Capron 8207F)	$\bar{M}_n$ = 25 000[b]	1.00	Allied Signal Inc.
MXD6	Poly(*m*-xylene adipamide) (MXD6 6007)	$\bar{M}_n$ = 25 300[c]	0.42	Mitsubishi Gas Chemical Co.
SEBS	Styrene–(ethylene/butene)–styrene (Kraton G 1652)	Styrene block = 7000 EB block = 37 500	1.33	Shell Chemical Co.
SEBS-*g*-MA	Styrene–(ethylene/butene)–styrene grafted with 1.84% maleic anhydride[d] (Kraton G 1901X)	Not available	0.84	Shell Chemical Co.

[a]Brabender torque at 260°C and 60 rev min^{-1} after 10 min divided by that of nylon-6
[b]Theoretical end-group analysis: 40 μeq/g NH_2 and 40 μeq/g COOH
[c]End-group analysis: 12 μeq/g NH_2 and 67 μeq/g COOH
[d]Determined by elemental analysis after solvent/non-solvent purification

BINARY MIXTURES OF NYLON-6 AND MXD6

Homogeneous polyamide mixtures

As described more fully elsewhere[1], mixing of nylon-6 and MXD6 by one pass through a single-screw extruder at 290°C causes sufficient interchange reactions to lead to phase homogenization in the melt and to a solid material with a single glass transition temperature. The latter point is evident from the d.m.t.a. data shown in *Figure 1*. The single tan δ peak associated with the glass transition region shifts monotonically with composition from the T_g of nylon-6 to that of MXD6. Nylon-6 has a prominent sub-T_g relaxation peak at about -50°C that is associated with local modes of main-chain motion[24]. The much weaker peak in this region for MXD6 is understandable in view of the presence of the rigid

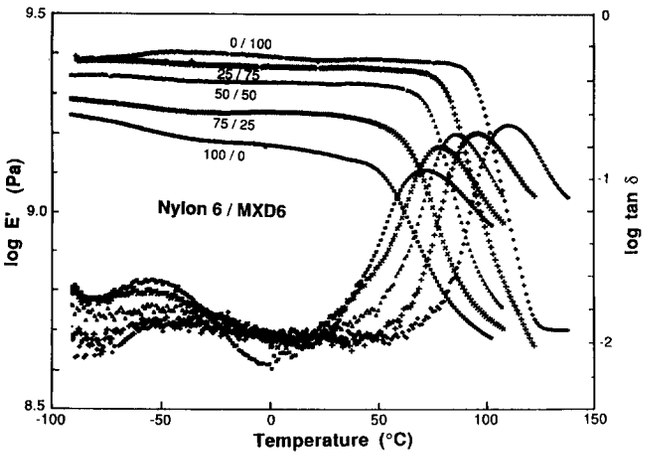

Figure 1 D.m.t.a. scans for melt-phase-homogenized nylon-6/MXD6 mixtures at 1 Hz and heating rate 2°C min^{-1}. The tan δ curves show similar progression with composition near the peak maximum as the modulus curves

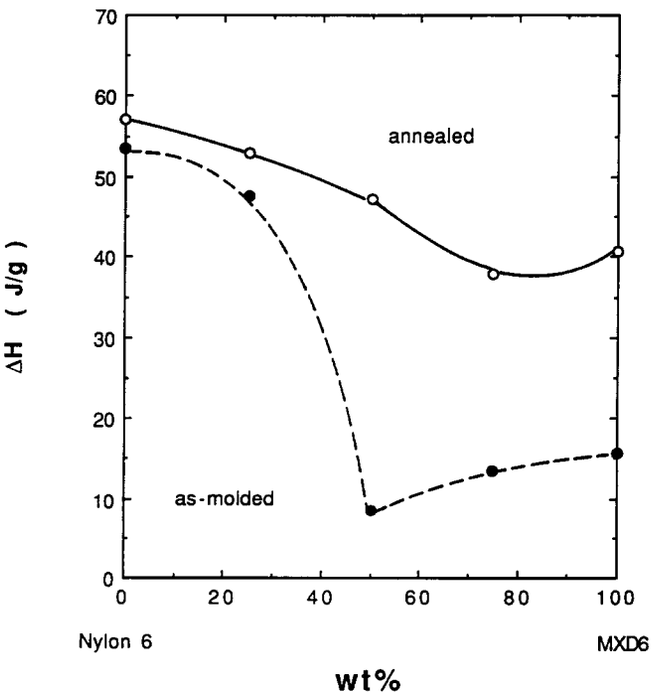

Figure 2 Total heat of fusion of homogeneous nylon-6/MXD6 mixtures (first heat of moulded samples). The broken curve is for as-moulded samples and the full curve is for samples annealed at 100°C for 12 h

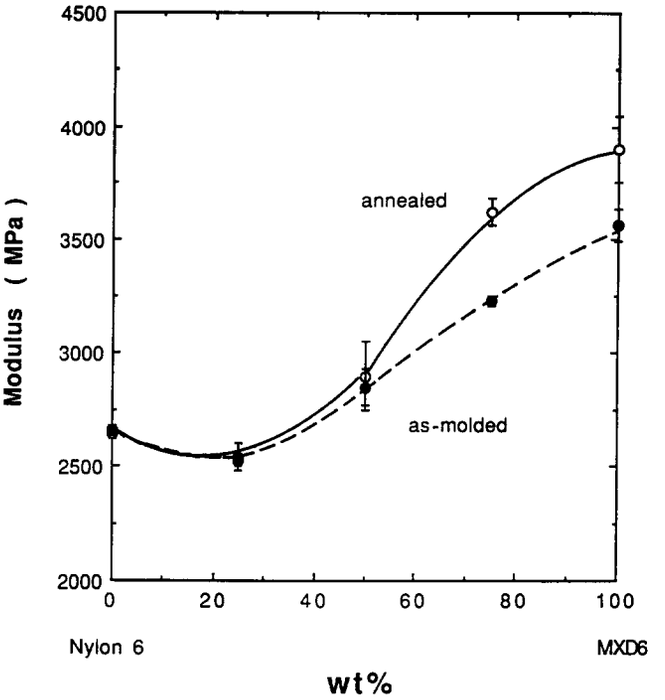

Figure 3 Tensile moduli of melt-phase-homogenized nylon-6/MXD6 mixtures. The broken curve is for as-moulded samples and the full curve is for samples annealed at 100°C for 12 h

phenylene groups and the lower concentration of flexible methylene groups in its repeat unit relative to nylon-6. The height of the tan δ peak at -50°C decreases continuously as the content of MXD6 increases. Because of the long sequences of nylon-6 and MXD6 units that persist after melt phase homogenization[1], both types of units are able to crystallize on cooling, albeit with separate melting points. *Figure 2* shows the combined heats of fusion for both crystal types for as-moulded and annealed melt-phase-homogenized nylon-6/MXD6 mixtures. As indicated by the ΔH values for as-moulded (mould temperature = 80°C) specimens, there is evidently some reduction of crystallization rates caused by either the interchange reactions or phase homogenization[1]. However, for annealed samples, the total heat of fusion increases and tends to follow the additive line more closely. The retention of a relatively high crystallizability for these mixed materials leads to higher levels of stiffness, strength and heat resistance than would be expected if the extent of interchange reaction led to more nearly random copolymer structures.

Figures 3 and *4* show the modulus and yield strength of phase-homogenized nylon-6/MXD6 mixtures directly after injection moulding at 260°C (minimal further interchange reaction) and after subsequent annealing. Both modulus and yield strength increase as a result of annealing, which is reasonable, at least simplistically, because this raises the overall level of crystallinity. However, these properties do not show simple additivity as composition is varied. Minima are seen at 75% nylon-6, which is interesting since the minimum in total crystallinity occurs at 75% MXD6. Evidently the property response reflects a complex phase morphology that, in the simplest case, consists of nylon-6 crystals, MXD6 crystals and a homogeneous amorphouse phase. Recent studies[25–28] have suggested even more complex structures for miscible blends of crystallizable polymers,

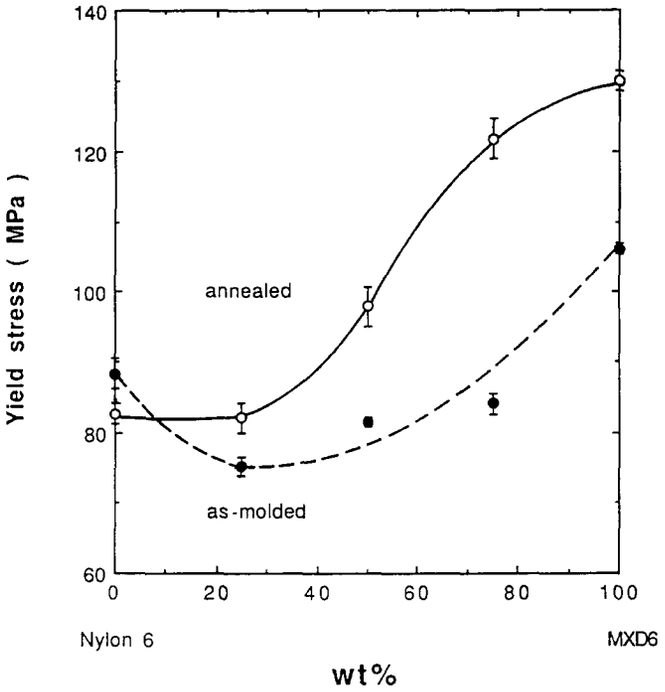

Figure 4 Tensile yield stress of melt-phase-homogenized nylon-6/MXD6 mixtures. The broken curve is for as-moulded samples and the full curve is for samples annealed at 100°C for 12 h

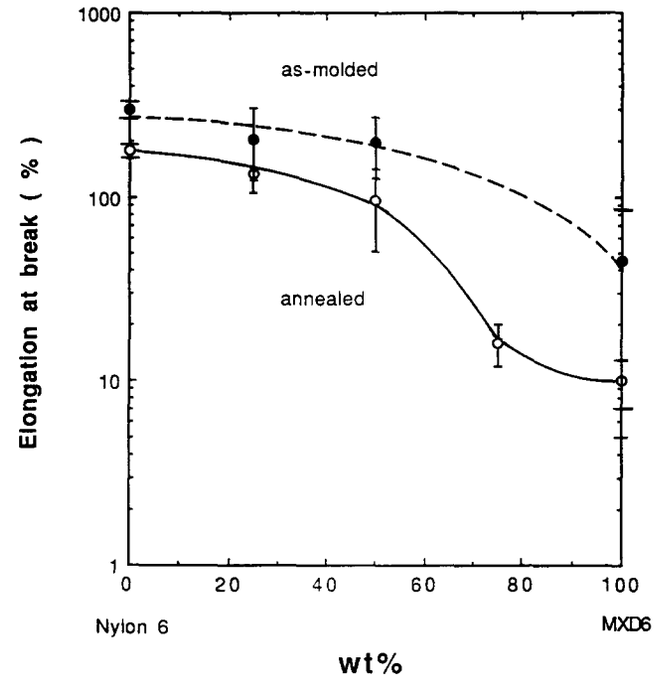

Figure 5 Elongation at break of melt-phase-homogenized nylon-6/MXD6 mixtures. The broken curve is for as-moulded samples and the full curve is for samples annealed at 100°C for 12 h

and such issues are equally likely to prevail in the present case. At this point there is no basis for any further attempts to rationalize the responses shown in *Figures 3* and *4*.

The elongation at break is shown in *Figure 5* for the same materials. As might be expected from its more flexible repeat unit and larger sub-T_g tan δ peak, nylon-6 is more ductile than MXD6 ahd has a higher elongation at break. Interestingly, melt-phase-homogenized mixtures of the two have elongations at break that are better than additive, at least on the scale used in *Figure 5*. Annealing reduces elongation at break presumably because of the associated increase in crystallinity, which is greater the higher the MXD6 content, and attendant changes in crystalline texture. The data for the as-moulded samples showed a large variation from sample to sample as the MXD6 content increased. This scatter was significantly reduced by the annealing procedure. In practice, these benefits of annealing may be achieved through optimization of moulding conditions.

Figure 6 shows the Izod impact strength of melt-phase-homogenized mixtures of nylon-6 and MXD6 after annealing. As expected, these data show that MXD6 is less tough than nylon-6. Interestingly, the impact strength of the mixtures closely parallels the magnitude of their tan δ peak heights at $-50°C$[29–31].

Heterogeneous polyamide mixtures

Heterogeneous nylon-6/MXD6 mixtures were prepared by extrusion at 260°C. *Figure 7* compares the combined heats of fusion for the two melting peaks of these heterogeneous mixtures, after annealing, with similar results for the phase-homogenized mixtures. At each composition, the heterogeneous materials have a higher ΔH, which in some cases is even above the additive line. The indicated loss in ΔH after phase homogenization tends to cause some softening, as may be seen by the comparison of moduli in *Figure 8* and yield stress in *Figure 9*. The elongation at break, however, is significantly higher for the homogeneous mixtures than the heterogeneous ones. Differences in crystallinity no doubt contribute partially to this manifestation of ductility; however, the basic incompatibility of the nylon-6/MXD6 pair is probably a dominant factor. The heterogeneous blend containing only 25% MXD6 has the same elongation at break as pure MXD6, yet the ΔH for the homogeneous and heterogeneous mixtures are nearly the same for this composition (*Figure 10*). In summary, phase homogenization causes significant

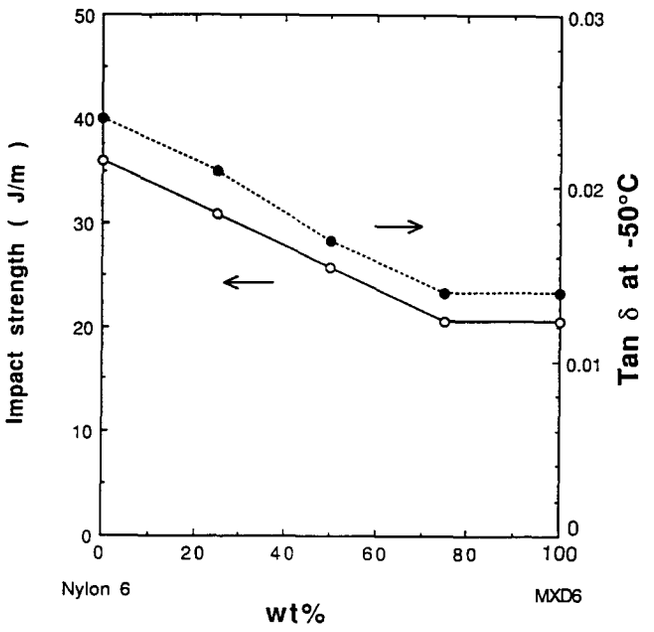

Figure 6 Notched Izod impact strength (solid line) and peak intensity of tan δ at $-50°C$ (dotted line) for melt-phase-homogenized nylon-6/MXD6 mixtures annealed at 100°C for 12 h

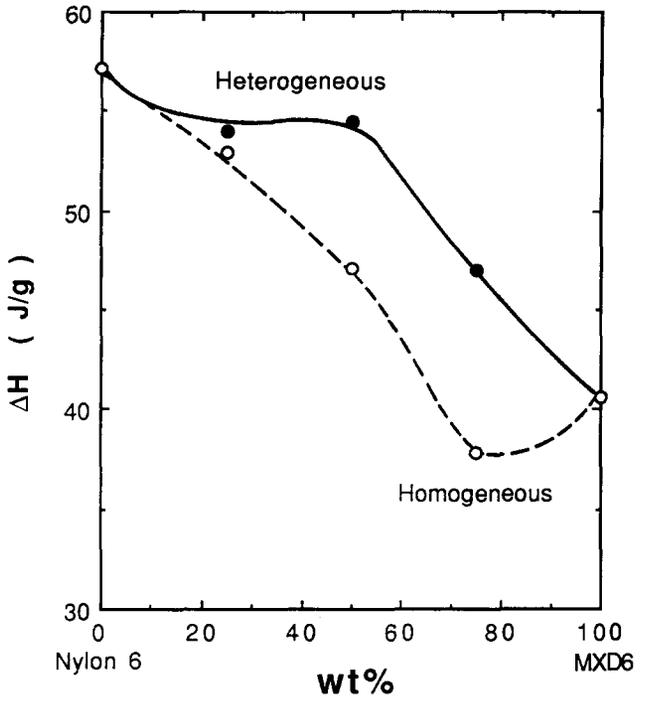

Figure 7 Total heat of fusion of nylon-6/MXD6 mixtures (first heat of moulded samples annealed at 100°C for 12 h). The full curve is for heterogeneous mixtures and the broken curve is for melt-phase-homogenized mixtures

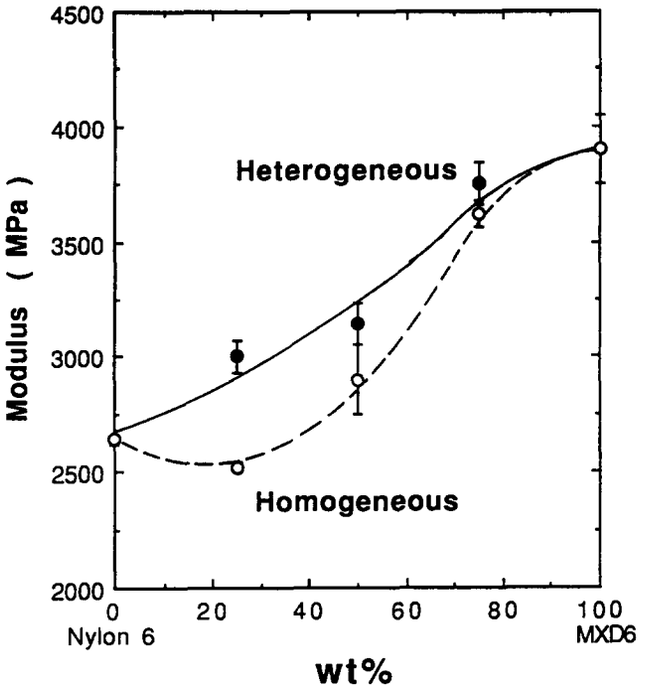

Figure 8 Tensile moduli of nylon-6/MXD6 mixtures annealed at 100°C for 12 h. The full curve is for heterogeneous mixtures and the broken curve is for melt-phase-homogenized mixtures

increases in ductility with some loss in stiffness and strength compared to the relatively more incompatible heterogeneous mixtures.

TERNARY MIXTURES OF NYLON-6, MXD6 AND SEBS-*g*-MA

Rheology

As judged by Brabender torque rheometry, the nylon-6 used here is more than twice as viscous as the MXD6 (see *Table 1*) at 260°C. SEBS is slightly more viscous than nylon-6, while the functionalized version, SEBS-*g*-MA, is slightly less so. Both elastomers are more viscous than MXD6. *Figure 11* shows the torque as a function of composition for melt-phase-homogenized nylon-6/MXD6 mixtures. The response is nearly additive for these binary compositions. Addition of SEBS-*g*-MA to nylon-6 causes a dramatic increase in torque owing to

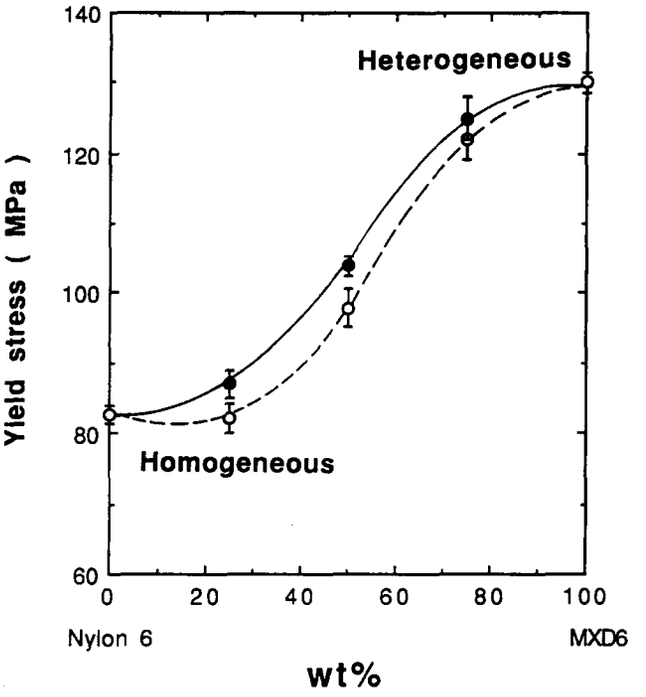

Figure 9 Tensile yield stress of nylon-6/MXD6 mixtures annealed at 100°C for 12 h. The full curve is for heterogenous mixtures and the broken curve is for melt-phase-homogenized mixtures

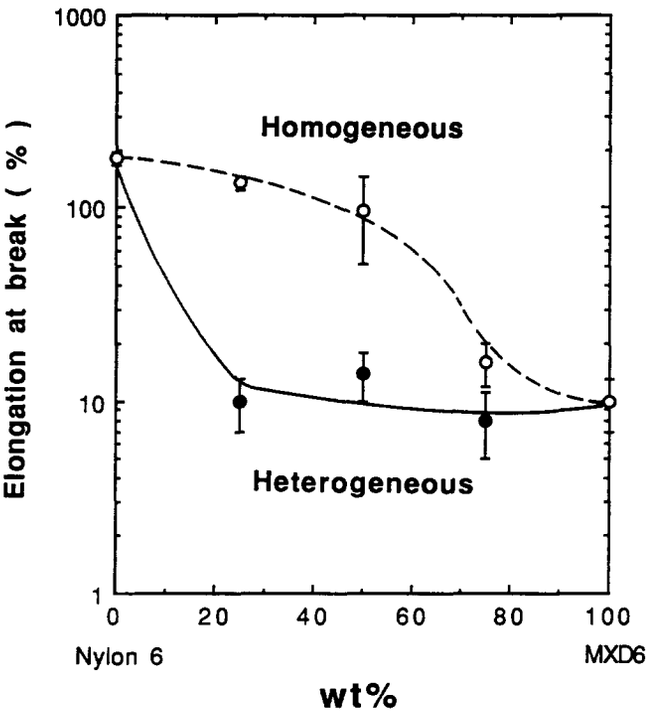

Figure 10 Elongation at break of nylon-6/MXD6 mixtures annealed at 100°C for 12 h. The full curve is for heterogeneous mixtures and the broken curve is for melt-phase-homogenized mixtures

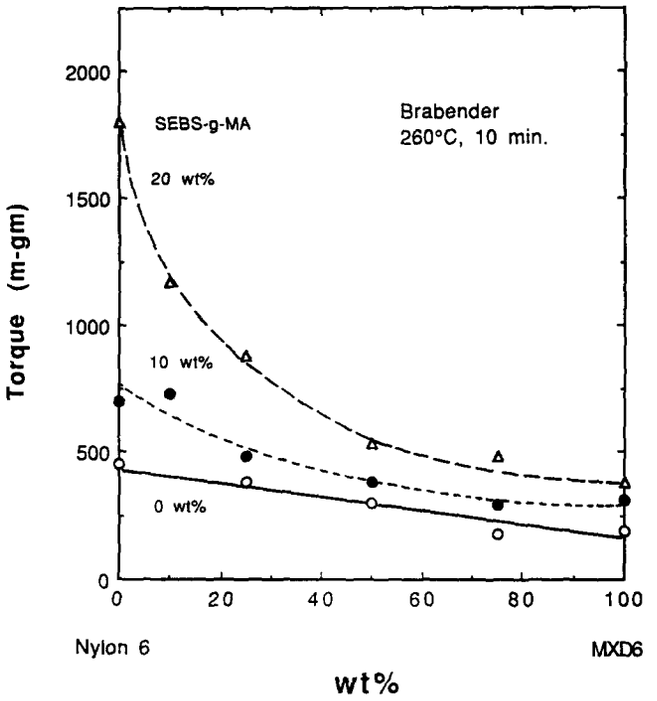

Figure 11 Brabender torque of melt-phase-homogenized polyamide mixtures/SEBS-*g*-MA blends after 10 min at 260°C and 60 rev min^{-1}

grafting of nylon-6 chains to the maleic-anhydride-containing elastomer as described earlier[3]. The increase in torque upon adding SEBS-*g*-MA to MXD6 is much less dramatic by comparison. Earlier[3,4] we suggested that nylon-6,6 tends to graft less effectively to SEBS-*g*-MA than does nylon-6, probably because of surface area differences. The torque increment found here for MXD6 is even less than that for nylon-6,6. The torque curves shown in *Figure 11* for mixtures containing 10 and 20% SEBS-*g*-MA are considerably below that expected from simple additivity. As described later, the morphology of nylon-6/SEBS-*g*-MA is dramatically changed by blending with MXD6, and these observations are probably closely interrelated.

Mechanical properties

As reported recently[3] blends of SEBS-*g*-MA with nylon-6 are not supertough because the rubber particles are evidently too small ($\sim 0.05\ \mu m$) for effective toughening. *Figure 12* shows that MXD6 is barely toughened at all by blending with SEBS-*g*-MA even though the rubber particles are more nearly of the size that toughens nylon-6 and nylon-6,6[3,4], as will be seen later. We speculate that MXD6 lacks the inherent ductility required for efficient rubber toughening. On the other hand, melt-phase-homogenized mixtures of nylon-6 and MXD6 are supertoughened by addition of 20% SEBS-*g*-MA. *Figure 12* shows a maximum in room-temperature notched Izod impact strength when the homogenized mixture of nylons contains about 10% MXD6. At 10% SEBS-*g*-MA, all samples showed brittle fracture; however, a maximum in impact strength is still observed at about 10% MXD6 in the nylon phase. Mixtures of nylon-6 and MXD6 blended under conditions (260°C extrusion temperature) that do not lead to melt phase homogenization are not significantly toughened by addition of 20% SEBS-*g*-MA, as seen in *Figure 13*.

Tensile properties are shown in *Figures 14–16* for melt-phase-homogenized nylon-6/MXD6 mixtures containing various levels of SEBS-*g*-MA. As expected, modulus and yield strength decrease as SEBS-*g*-MA is added, while elongation at break increases. As the content of MXD6 in the nylon phase increases, modulus and yield strength increase, while elongation at break decreases.

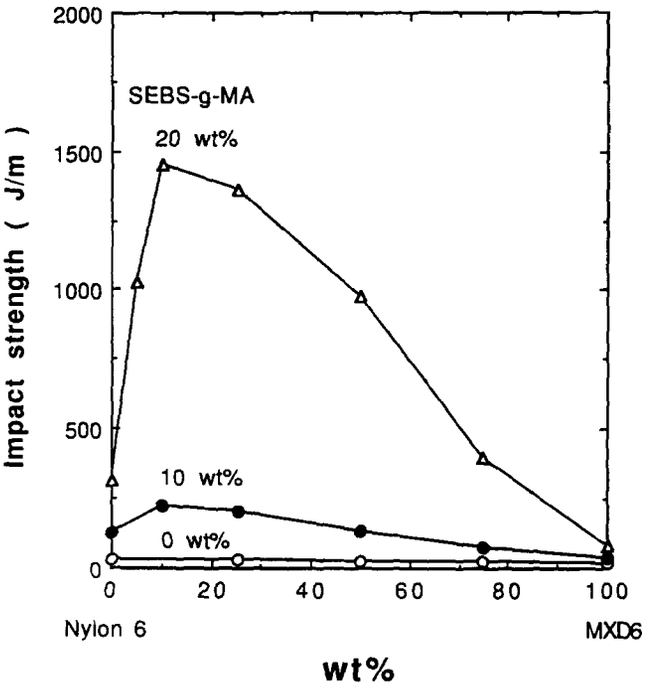

Figure 12 Notched Izod impact strength for melt-phase-homogenized polyamide mixtures containing various amounts of SEBS-*g*-MA after annealing at 100°C for 12 h. Error limits of these values are within ±5%

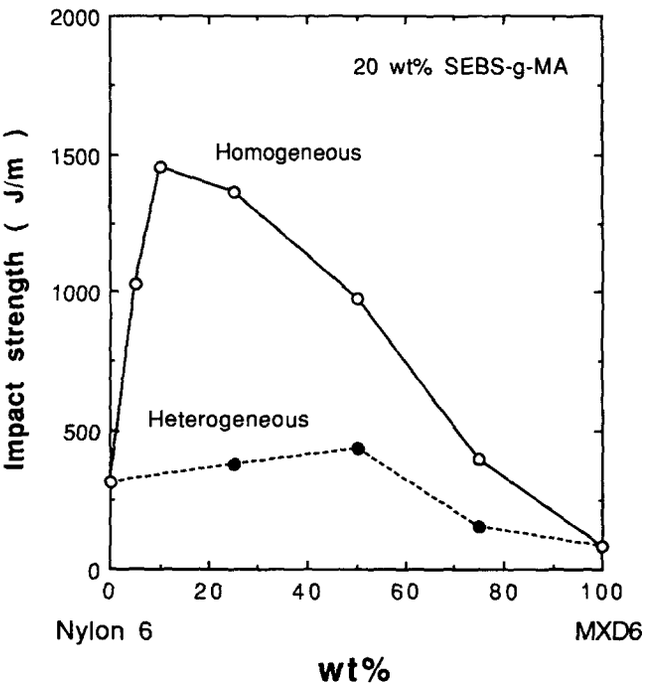

Figure 13 Notched Izod impact strength of 80/20 polyamide/SEBS-*g*-MA blends annealed at 100°C for 12 h. Dotted line is for heterogenous polyamide phase and full line is for melt-phase-homogenized polyamide phase

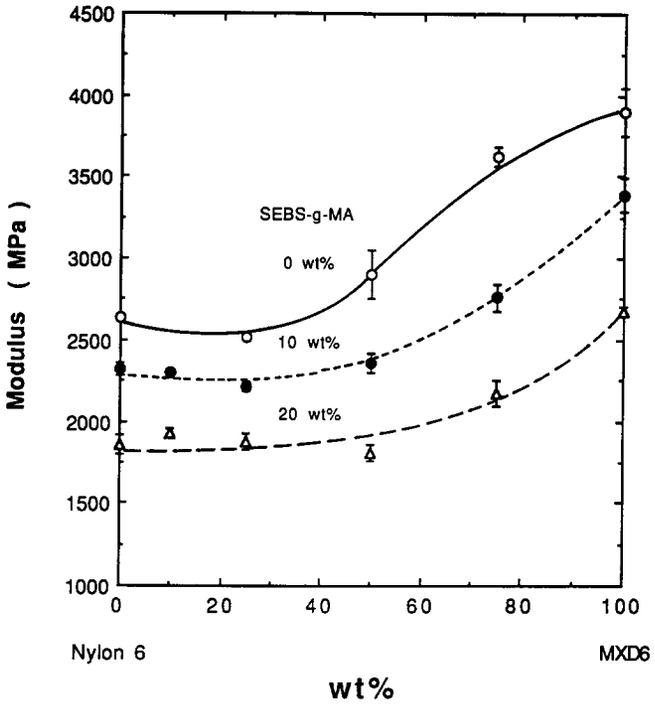

Figure 14 Tensile modulus for melt-phase-homogenized polyamide mixtures containing various amounts of SEBS-*g*-MA after annealing at 100°C for 12 h

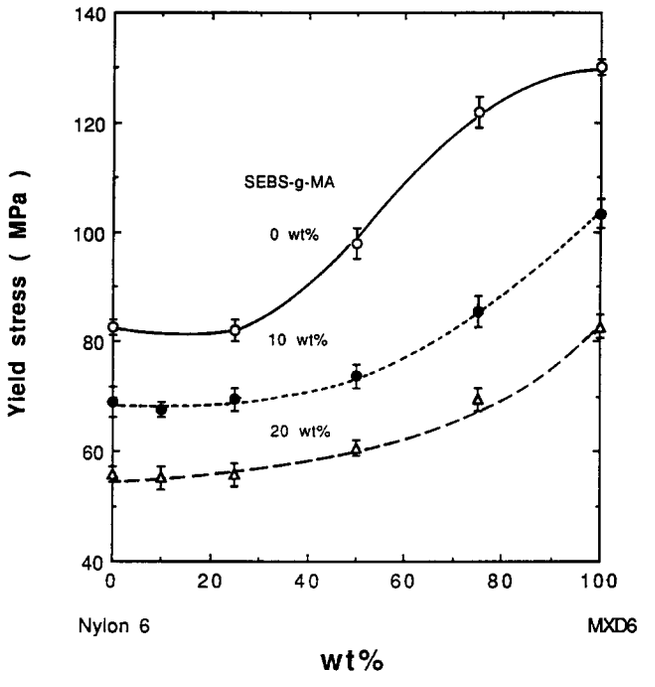

Figure 15 Tensile yield stress for melt-phase-homogenized polyamide mixtures containing various amounts of SEBS-*g*-MA after annealing at 100°C for 12 h

More detailed studies of impact behaviour were performed on melt-phase-homogenized mixtures containing 75% nylon-6 and 25% MXD6. *Figure 17* shows the notched impact strength as a function of impact velocity (measured using the Dynatup apparatus rather than the standard Izod test) for blends with varying levels of SEBS-*g*-MA. Ductile–brittle transition velocities are seen within the range tested for blends containing 10 and 15% SEBS-*g*-MA. The blend containing 20% is supertough at all velocities tested. Note that the velocity in the standard Izod test (see *Figure 12*) is 3.4 m s^{-1}.

Figure 18 shows standard Izod impact strengths as a function of test temperature for homogenized 75/25 nylon-6/MXD6 mixtures containing varying amounts of SEBS-*g*-MA. The ductile–brittle transition temperatures obtained from these results are plotted in *Figure 19* as a function of the content of SEBS-*g*-MA. The dotted line represents results from Gaymans *et al.*[9,11] for nylon-6 toughened by a maleic-anhydride-functionalized ethylene/propylene elastomer, EPR-*g*-MA. The difference between the nylon-6/EPR-*g*-MA and nylon-6/MXD6/SEBS-*g*-MA blends may stem from several causes. First, the presence of MXD6 units in the matrix no doubt has some influence. Secondly, the elastomer phases differ

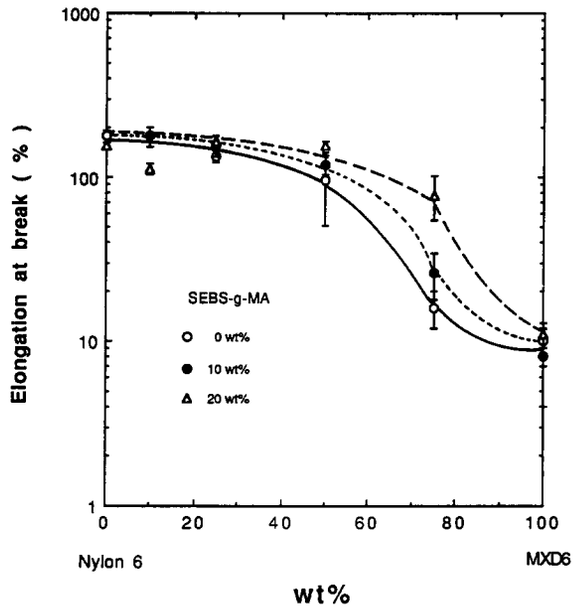

Figure 16 Elongation at break for melt-phase-homogenized polyamide mixtures containing various amounts of SEBS-*g*-MA after annealing at 100°C for 12 h

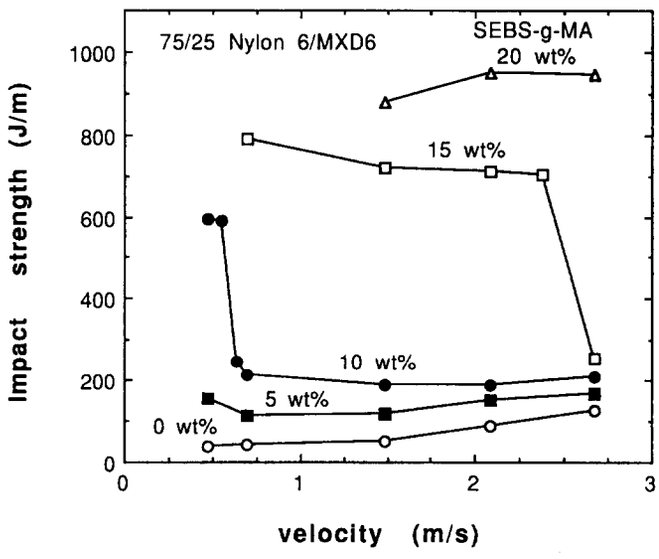

Figure 17 Dynatup impact strength *versus* impact velocity for melt-phase-homogenized polyamide mixtures (75/25 nylon-6/MXD6) containing various amounts of SEBS-*g*-MA after annealing at 100°C for 12 h

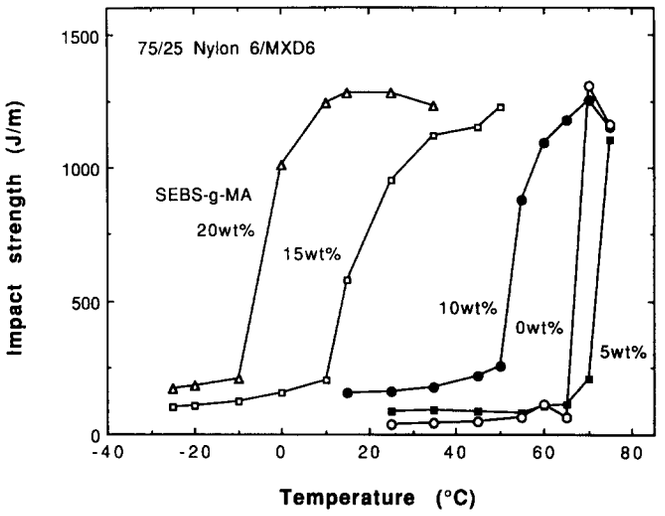

Figure 18 Notched Izod impact strength as a function of temperature for melt-phase-homogenized polyamide mixtures (75/25 nylon-6/MXD6) containing various amounts of SEBS-*g*-MA after annealing at 100°C for 12 h

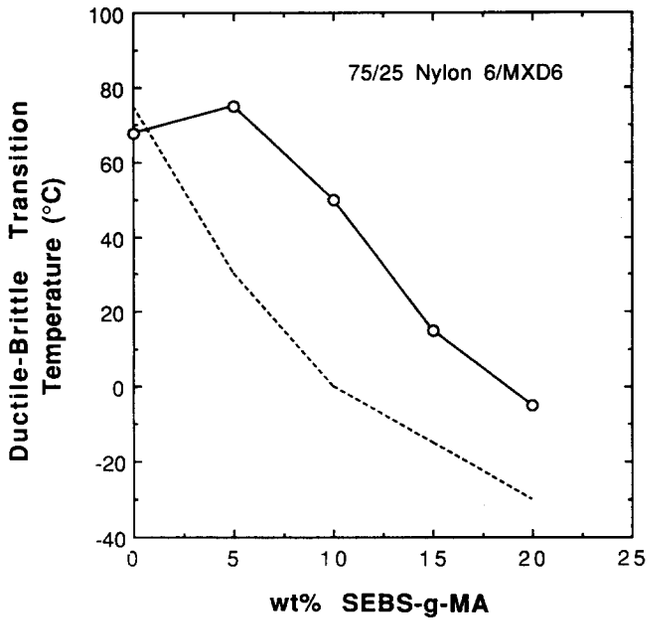

Figure 19 Ductile–brittle transition temperature from *Figure 18* as a function of SEBS-*g*-MA composition. The dotted line shows data for nylon-6/EPR-*g*-MA blends[8]

in ways that may be fundamentally important. Finally, particle size apparently influences the ductile–brittle transition temperature[9,11]; hence, comparable morphologies need to be compared in order to assess questions about the influence of matrix or elastomer characteristics on the ductile–brittle transition temperature. For the current system, there seems to be a curious increase in the ductile–brittle transition temperature before it eventually decreases with further addition of elastomer.

Phase-homogenized mixtures of 75/25 nylon-6/MXD6 were blended with mixtures of SEBS and SEBS-*g*-MA to give compositions containing 20% rubber. *Figure 20* shows the Izod impact strength of these blends as a function on the content of elastomer type. When the rubber phase contains 10% or less of SEBS-*g*-MA, the blends undergo brittle fracture. When the content of SEBS-*g*-MA is 25% or more of the elastomer phase, the blends are supertough. There is a ductile–brittle transition between these limits. Based on the previous work[3,4], dramatic changes in morphology can be expected as the proportion of the two rubbers varies. No doubt, at high SEBS content the particles become too large and their adhesion to the matrix may be insufficient for toughening.

Ternary blends can be prepared by a number of different mixing protocols[3,4,32] involving multiple extrusion steps. In the present system, the point at which phase homogenization of the two polyamide components is attempted, if at all, is another variable. *Table 2* gives a brief examination of this issue. Measures of ductility (Izod impact and elongation at break) are compared for a single composition, 75/25 nylon-6/MXD6 plus 20% SEBS-*g*-MA, prepared in four different ways. These procedures should lead to homogeneous (samples A and C) or heterogeneous (samples B and D) polyamide melt phases. For samples A and B, the polyamides were extruded at 290 and 260°C, respectively, and then compounded with 20 wt% SEBS-*g*-MA at 260°C. For samples C and D, 80/20 nylon-6/SEBS-*g*-MA and 80/20 MXD6/SEBS-*g*-MA blends were separately prepared at 260°C and then these blends were extruded at 290 and 260°C, respectively. The blends that include the 290°C homogenization step were supertough and have high elongations at break irrespective of blending method. The blends without the 290°C homogenization step invariably show much lower ductility. Blends of SEBS-*g*-MA with a heterogeneous polyamide mixture may be brittle for several reasons. First, SEBS-*g*-MA does not toughen nylon-6, because the particles are too small[3], nor does it toughen MXD6, evidently because of the inherent brittleness of this matrix, as seen in *Figure 12*. Thus, neither phase is tough in such mixtures. Furthermore, there is the inherent incompatibility of heterogeneous mixtures of nylon-6 and MXD6 as suggested earlier. It is interesting to note that extrusion at 290°C seems to

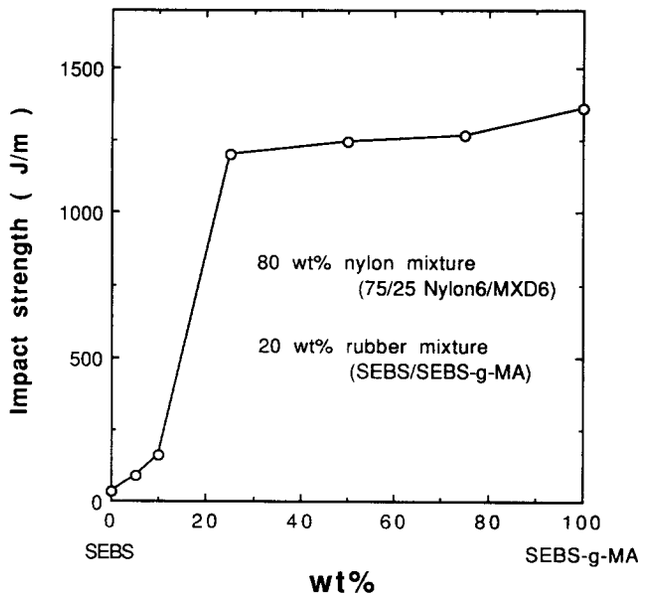

Figure 20 Notched Izod impact strength of melt-phase-homogenized polyamide mixtures (75/25 nylon-6/MXD6) blended with varying ratio of SEBS/SEBS-*g*-MA in the elastomer phase (total rubber = 20 wt%). Blends annealed at 100°C for 12 h

Table 2 Effect of mixing protocol[a] on toughness of nylon-6/MXD6/SEBS-*g*-MA 60/20/20 blends having homogeneous and heterogeneous polyamide phases

Polyamide phase	Sample A, homogeneous	Sample B, heterogeneous	Sample C, homogeneous	Sample D, heterogeneous
Impact strength (J m^{-1})	1360	380	1160	470
Elongation at break (%)	170	60	150	70

[a]Sample preparation:
Sample A 1st extrusion – 75/25 nylon-6/MXD6 at 290°C
2nd extrusion – 80/20 nylon mixture/SEBS-*g*-MA at 260°C
Sample B 1st extrusion – 75/25 nylon-6/MXD6 at 260°C
2nd extrusion – 80/20 nylon mixture/SEBS-*g*-MA at 260°C
Sample C 1st extrusions – 80/20 nylon-6/SEBS-*g*-MA and 80/20 MXD6/SEBS-*g*-MA at 260°C
2nd extrusion – 75/25 (nylon-6/SEBS-*g*-MA blend)/(MXD6/SEBS-*g*-MA blend) at 290°C
Sample D 1st extrusions – 80/20 nylon-6/SEBS-*g*-MA and MXD6/SEBS-*g*-MA at 260°C
2nd extrusion – 75/25 (nylon-6/SEBS-*g*-MA blend)/(MXD6/SEBS-*g*-MA blend) at 260°C

rectify these problems through phase homogenization, whether this is done before or after mixing with the rubber.

Morphology

Figure 21 shows transmission electron photomicrographs of blends containing 20% SEBS-*g*-MA whose homogenized polyamide phase varies in composition from pure nylon-6 to pure MXD6. For the pure nylon-6 matrix (*Figure 21a*), the elastomer particles are very finely dispersed (weight-average particle diameter ~ 0.06 μm), as previously reported[3,6]. Such small particles are evidently not able to produce very significant toughening of nylon-6[3,33]. On the other hand, the elastomer particles are much larger, $d_w \sim 0.30$ μm, when the matrix is pure MXD6 (see *Figure 21e*). Most of the particles are nearly spherical but many have complex, irregular shapes and occlusion of matrix material in the elastomer phase is common. The morphology of the MXD6-based blend is reminiscent of that recently reported[4] for corresponding blends having nylon-6,6 as the matrix. In the case of the latter, the rubber particles were even more irregular in shape but quite similar in size. It could be argued that rheological factors play some role in these morphological differences. As shown in *Table 1*, SEBS-*g*-MA is slightly less viscous than nylon-6 but is twice as viscous as MXD6 based on the Brabender torques reported here. However, we feel that this is not enough to produce the order-of-magnitude difference in morphology shown in *Figures 21a* and *21e*, and what follows will reinforce this view.

In a previous paper[4], we proposed that there is a key difference in the reactions of nylon-6 and nylon-6,6 with maleated materials. Nylon-6, like its monomer in the ring-open state, is always monofunctional in each of the two types of functional groups, $-NH_2$ or –COOH. Thus, there is only one amine end-group for reaction with anhydrides. In principle, amide linkages may also react with anhydrides[17,19,21], and in this case nylon-6 is also monofunctional, i.e. each nylon-6 chain can only have one point of attachment to an anhydride-functionalized polymer molecule or phase. On the other hand, nylon-6,6 molecules, also like the monomers it is made from, can be difunctional with respect to either $-NH_2$ or –COOH. Whether the reaction with anhydride units involves amine ends or amide units, it is possible for nylon-6,6 molecules to have two points of attachment to an anhydride-functionalized polymer molecule or phase. In this regard, MXD6 is like nylon-6,6 rather than nylon-6.

Because nylon-6 undergoes single end-grafting to the anhydride-functionalized phase, there will be a decrease in interfacial tension and stabilization against coalescence. Thus, the elastomer phase forms small particles, i.e. it is effectively emulsified. Because of the difunctionality of nylon-6,6 and MXD6, these molecules may attach twice on the same particle, i.e. loops, or form bridges between two rubber particles. The former can act to prevent particle break-up or separation, while the latter may encourage coalescence. Both may provide a mechanism for occlusion of matrix material into the rubber particles. If the reaction involves only amine ends, then some molecules will react like nylon-6 while others will not react at all since a certain distribution of the chains, depending on the balance of –COOH and $-NH_2$, will have two, one, or zero amine ends.

It is now interesting to consider the morphology of SEBS-*g*-MA blends with melt-phase-homogenized mixtures of nylon-6 and MXD6 (see *Figures 21b* to *21e*). None of these blends have the extremely small phase size seen when the matrix is nylon-6, but rather each has relatively larger particles of complex shape. When the matrix contains 75 wt% MXD6 (*Figure 21d*) the rubber particles are rather similar to those for the pure MXD6 matrix (*Figure 21e*). For the matrices containing 25 wt% (*Figure 21b*) and 50 wt% (*Figure 21c*) MXD6, the particles are even more complex in shape.

The complex shapes of the rubber particles make determination of an average size difficult; nevertheless, a quantitative analysis of the photomicrographs in *Figure 21* was attempted. The diameter assigned to each particle (including any occluded polyamide) was the average of its longest dimension and its dimension perpendicular to this major axis. *Figure 22* shows histograms for such measurements on 200 to 350 particles in each of the photomicrographs in *Figure 21*. In all cases there is a large number of small particles, but the distribution clearly skews to larger particles as the content of MXD6 increases. Weight-average particle diameters were calculated via:

$$\bar{d}_w = \frac{\sum n_i d_i^2}{\sum n_i d_i} \quad (1)$$

These are plotted *versus* MXD6 content in *Figure 23*. This measure of size increases from 0.06 μm for nylon-6 via a sigmoidal-type curve to a value of 0.3 μm for MXD6. As mentioned earlier, Wu[7,8] has proposed that the interparticle distance, τ, is a more fundamental criterion for toughening than particle size *per se*. The average

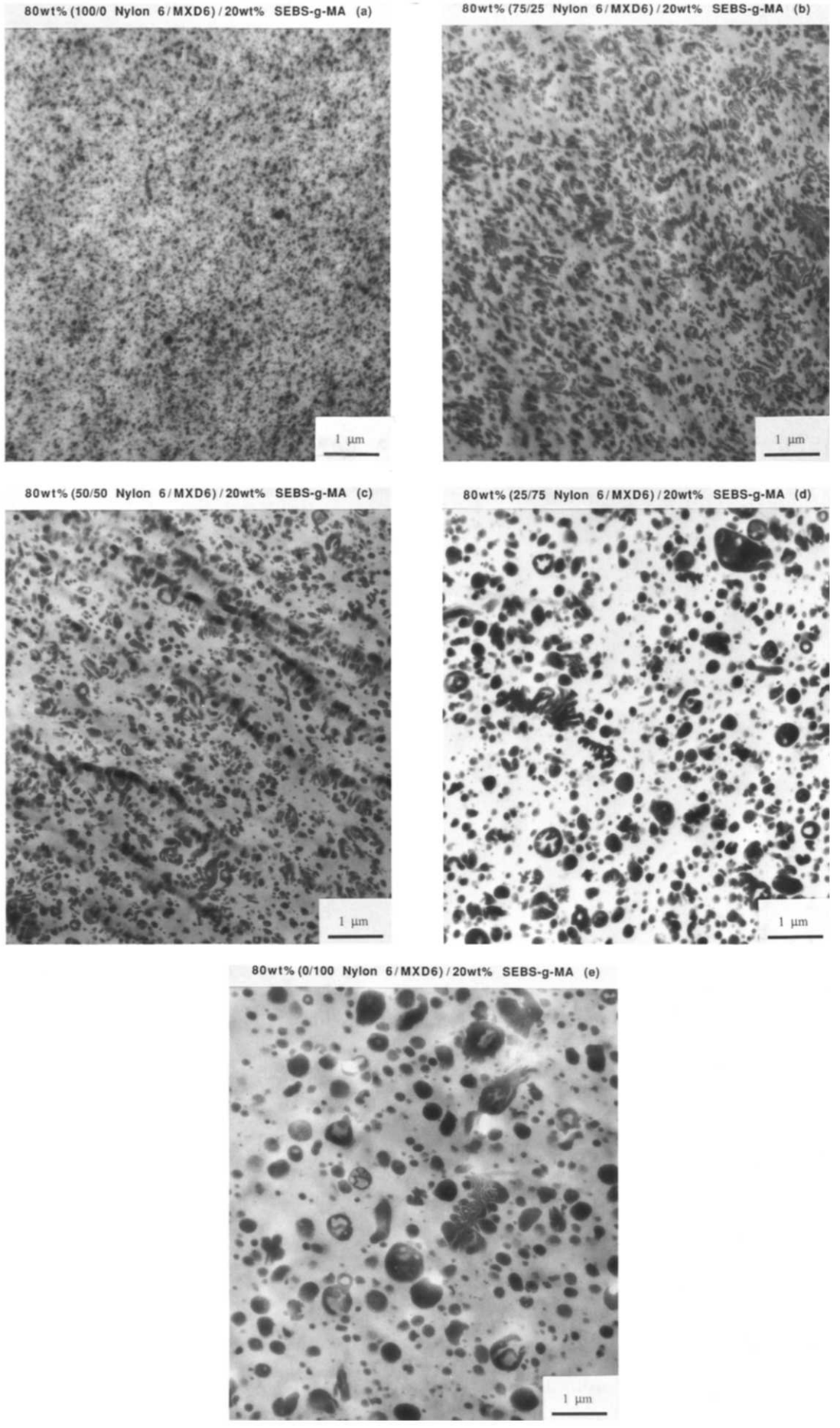

Figure 21 TEM photomicrographs for melt-phase-homogenized polyamide mixtures containing 20 wt% SEBS-*g*-MA as a function of nylon-6/MXD6 ratio

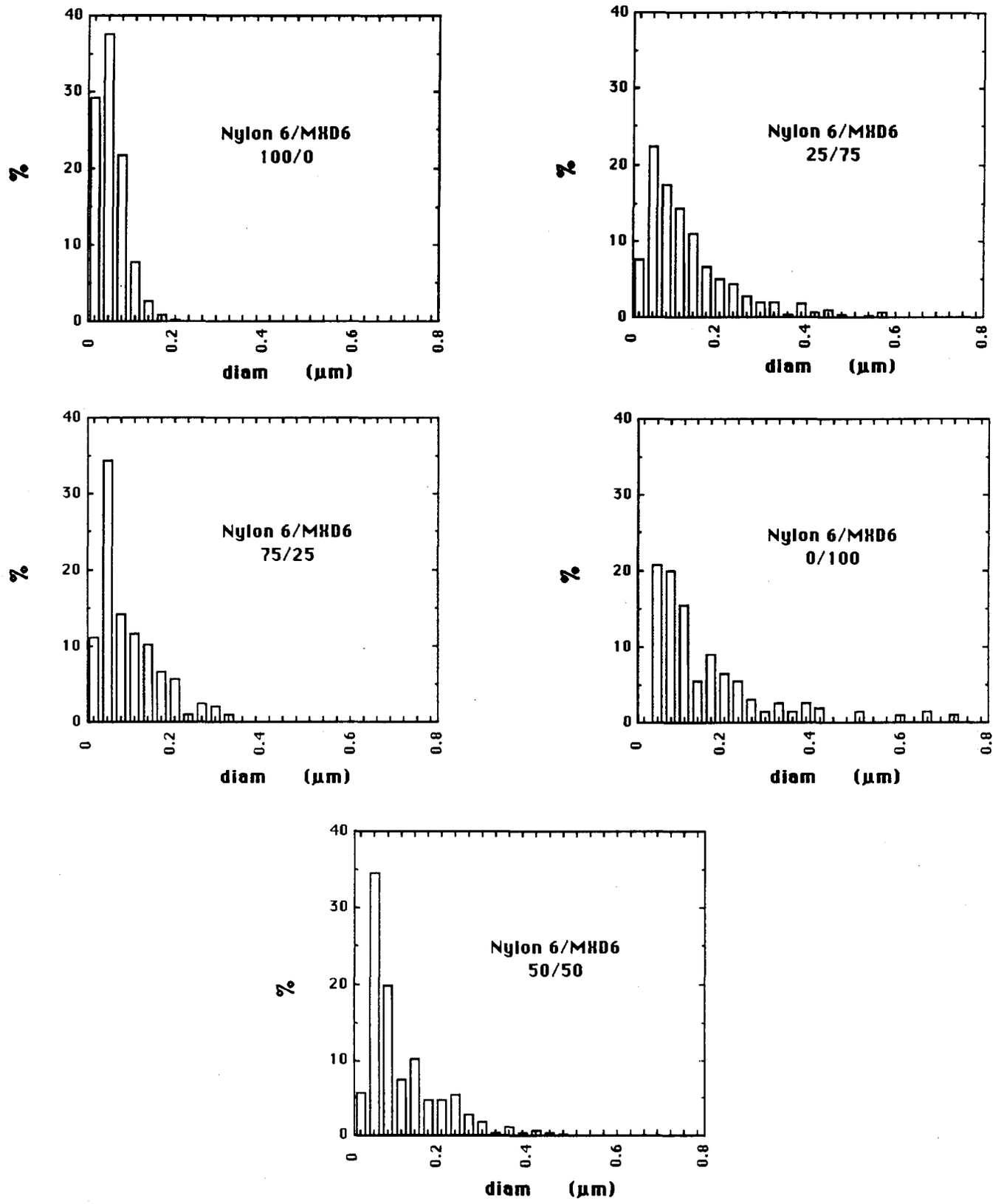

Figure 22 Rubber particle size distributions obtained from TEM photomicrographs in *Figure 21*

interparticle distances were estimated from the photomicrographs in *Figure 21* using two different procedures. In the first, several hundred adjacent rubber particle pairs were selected at random in each photomicrograph. A line was drawn between the centres of the two particles. The length of the fraction of this line that cut through the matrix was defined as the interparticle distance. The weight average of the set of values for each composition, $\bar{\tau}_w$, is plotted in *Figure 23*. The values show a remarkable parallel to the weight-average particle size, $\bar{d}_w$. The second approach is the one used by Wu, where all the rubber particles are assumed to have the same diameter and to be regularly arranged in space such that the interparticle distance can be calculated from the following

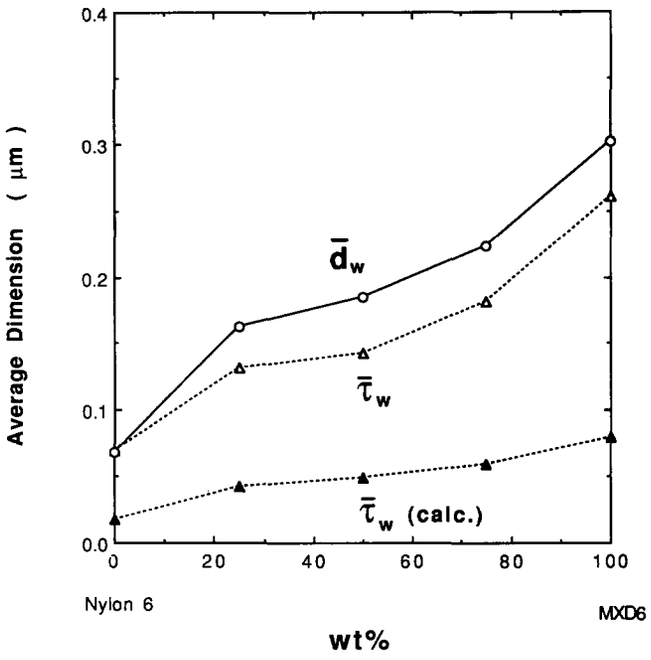

Figure 23 Weight-average particle diameter $\bar{d}_w$ and interparticle distance $\bar{\tau}_w$ obtained from TEM photomicrographs in *Figure 21*. $\bar{\tau}_w$(calc) is the interparticle distance calculated by equation (2)

formula derived from simple geometrical considerations:

$$\tau = [(\pi/6\phi)^{1/3} - 1]d \qquad (2)$$

where d is the uniform particle diameter and ϕ is the rubber phase volume fraction. For 20% rubber by weight, ϕ is approximately 0.26. For the present calculation, we used $\bar{d}_w$ in this formula and designated the calculated 'average' interparticle distance as $\bar{\tau}_w$(calc). As seen in *Figure 23*, the latter measure gives much smaller values than the former approach. The first method is probably the most realistic indicator of the actual interparticle distance.

The impact data in *Figure 12* and the particle sizes from *Figure 23* can be cross-plotted as shown in *Figure 24*. While there appears to be a maximum at an apparent optimum particle size, these results are quite different from the other data for nylon-6 with varying rubber particle diameter shown for comparison (broken lines). The basic features are retained if interparticle distance is substituted for $\bar{d}_w$ owing to the similarity of these two dimensions. Of course, the present data should not be thought of simply in terms of a critical rubber particle size or rubber interparticle distance, since in addition to the changes in morphology involved there is also a change in the nature of the polyamide matrix as MXD6 is added to nylon-6. We recently described an analogous problem for ABS (acrylonitrile–butadiene–styrene) systems and showed the need for accounting for the change in the inherent ductility of the matrix material itself[34]. In the present case, adding MXD6 does increase the rubber particle size but it also evidently reduces the inherent ductility of the polyamide matrix. The latter effect is probably more of a factor in the decrease in impact strength with increased particle size than is this change in dimension *per se*.

It appears that the optimum toughening shown in *Figures 12* for matrices based on melt-phase-homogenized mixtures of nylon-6 and MXD6 can be explained as follows. Nylon-6 containing 20% SEBS-*g*-MA is not toughened because the elastomer particles are too small[3,6]. MXD6 containing 20% SEBS-*g*-MA is not toughened because this matrix is inherently brittle. Phase homogenizing MXD6 with nylon-6 leads to a matrix that is more ductile than MXD6 alone and to blends with SEBS-*g*-MA that have particles or interparticle distances that are large enough (unlike nylon-6 alone) but not too large[3,7,8] for toughening. The larger particles caused by addition of the MXD6, in our opinion, stems from the difunctional character that the MXD6 introduces to the segmented block-like copolymers with nylon-6 that are created. In other words, nylon-6 segments add inherent ductility while MXD6 adds the chemical character to yield optimum-size rubber particles. Evidently only 5–10% MXD6 is needed to accomplish the latter, as seen in *Figure 12*. This speaks strongly against any significant influence of rheological factors on the morphology since so little MXD6 hardly changes the rheological character of nylon-6 (see *Figure 11*). Other examples of toughening of monofunctional/difunctional polyamide pairs will be discussed in the future.

It should be mentioned that the MXD6 used here has a relatively low content of amine end-groups compared to its carboxyl ends or the amine ends of the nylon-6. One might argue that this lower functionality is responsible for the results shown here if it is assumed that the reaction of polyamides with anhydrides is limited to amine chain ends. Further work is needed to determine more definitively whether the amide linkages participate in this reaction or not. If amide participation is ignored, it could be said that the rubber particle size increase, upon incorporation of MXD6 in the polyamide matrix, seen in *Figure 23* is caused by the resulting dilution of the amine end content of the nylon-6. It would be surprising if the large increase in impact strength seen in

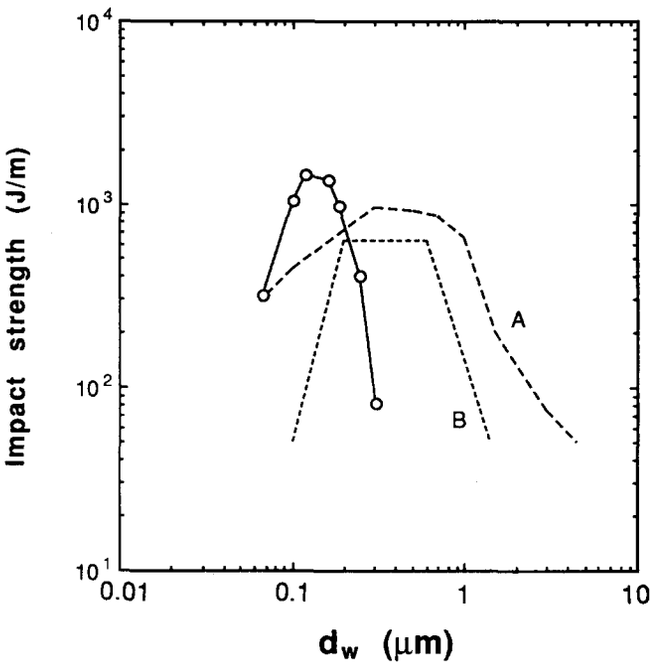

Figure 24 Notched Izod impact strength of melt-phase-homogenized polyamide mixtures containing 20 wt% SEBS-*g*-MA as a function of rubber particle size. The full line is drawn through the data from *Figure 23*. Broken lines A and B represent data for nylon-6/rubber blends reported by Oshinski *et al.*[3] and by Gaymans *et al.*[33]

Figure 12 upon adding only 10% MXD6 could be caused by such a minor dilution. Low amine content would also not explain the increased complexity in particle shape (in *Figure 21*) that results from addition of MXD6. The shape effects are more consistent with the arguments about difunctionality put forth above and in a previous paper[4]. Work in progress on use of nylon-6 and MXD6 with varying contents of amine end-groups will be more definitive about this issue, and the preliminary conclusions suggest that use of an MXD6 with a higher amine end-group content does not alter the trends shown here.

Thermal and dynamic mechanical anslysis

Figure 25 shows the heat of fusion for the phase-homogenized polyamide portion of blends containing various amounts of SEBS-*g*-MA. The values have been normalized per gram of polyamide in the blend, so for a given nylon-6/MXD6 ratio the results should be the same regardless of the SEBS-*g*-MA level, provided the latter does not influence the level of polyamide crystallinity. While there are some variations in this heat of fusion, it would be difficult to indicate any dominant role for crystallinity in the toughening of these nylon-6/MXD6/SEBS-*g*-MA mixtures.

As seen in *Figure 1*, nylon-6 has a fairly strong sub-T_g relaxation peak at about $-50°C$ while MXD6 has a much weaker peak in this region. The T_g of the EB mid-block phase of SEBS-*g*-MA also occurs in this region. Thus, it is interesting to examine the response of the composite of these various processes to blend composition. *Figure 26* shows the tan δ at the peak maximum for the ternary mixtures. Without any rubber present, the phase-homogenized MXD6/nylon-6 mixtures show a nearly monotonic curve connecting the values of nylon-6 and MXD6. This reflects the sub-T_g local mode motion in the matrix. Addition of SEBS-*g*-MA naturally causes a large increase owing to the mid-block rubber phase T_g. However, it is interesting to note that the lines of constant rubber content exhibit a maximum in tan δ at intermediate ratios of the matrix components near where toughness is maximum. This observation deserves further comment.

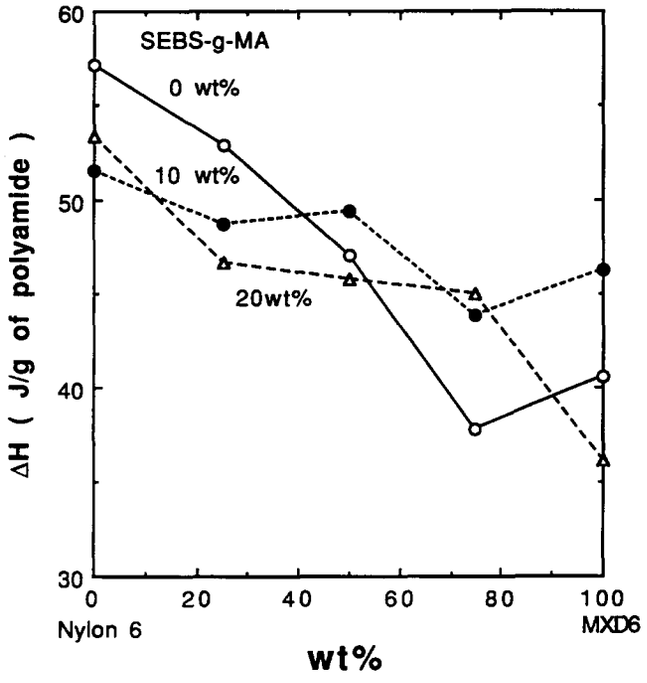

Figure 25 Heats of fusion of polyamide phase portion in melt-phase-homogenized polyamide mixtures blended with SEBS-*g*-MA. Samples annealed at 100°C for 12 h

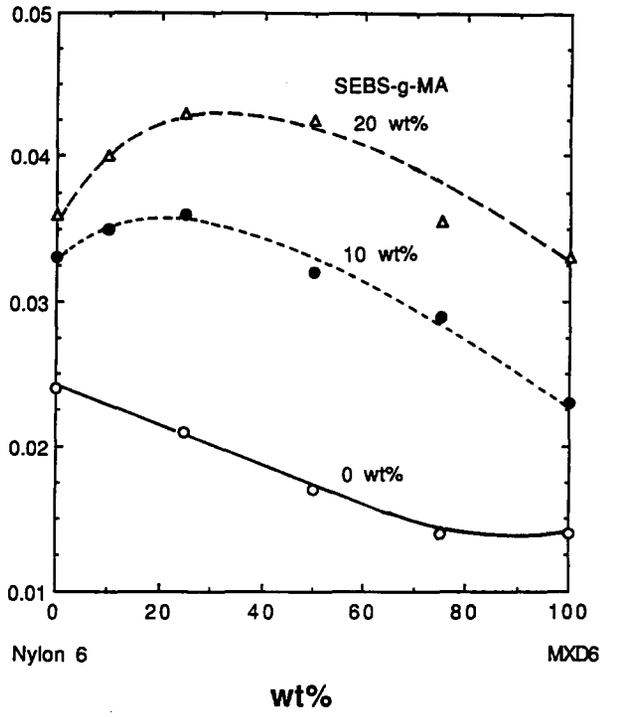

Figure 26 Tan δ peak intensity at peak maximum (near $-50°C$) for melt-phase-homogenized polyamide containing various amounts of SEBS-*g*-MA. Samples annealed at 100°C for 12 h

Table 3 Comparison of impact strength and loss peak of phase-homogenized 75/25 nylon-6/MXD6 mixtures containing 20% rubber consisting of varying proportions of SEBS and SEBS-*g*-MA

SEBS-*g*-MA (wt%) in rubber mixture	Impact strength ($J\ m^{-1}$)	Peak intensity of tan δ at $-50°C$
0	30	0.0470
25	1200	0.0435
50	1240	0.0435
75	1270	0.0430
100	1360	0.0430

Low-temperature tan δ peaks stemming from either the rubber or the matrix have often been discussed in the literature[12,13,35,36]. Any relationship between the magnitude of such peaks and impact strength is complicated and often not unique. The following factors may contribute to the maximum shown in *Figure 26*. In a previous paper[3] we showed that tan δ at $-50°C$ for nylon-6 blended with SEBS is higher than that blended with SEBS-*g*-MA. The grafting present and the much smaller particles in the latter case can both act to restrain elastomer phase motion (or damping) at its T_g. This effect is also seen in *Table 3*, where the matrix is a phase-homogenized mixture of 75/25 nylon-6/MXD6. Tan δ decreases as the rubber phase contains more SEBS-*g*-MA. Thus, in *Figure 26*, addition of MXD6 to

the matrix leads to a tendency for tan δ to increase because the rubber particles grow larger (and grafting extent is probably less). However, this trend is reversed eventually because of the decrease in tan δ of the matrix phase (see 0% SEBS-*g*-MA curve in *Figure 26*). Consequently, the maxima in tan δ shown in *Figure 26* may be, at least in part, fortuitous rather than actually forecasting the maximum in toughening seen in this region of composition.

CONCLUSIONS

As demonstrated previously[1], melt blending of nylon-6 and poly(*m*-xylene adipamide) (MXD6) can under certain conditions lead to a material with a homogeneous melt and a single T_g because of interchange reactions. The copolymer formed retains relatively long sequences of each polyamide type that are able to crystallize only slightly less than expected for a physical blend. Thus, these materials maintain nearly additive strength and stiffness characteristics without the problems expected of an incompatible physical blend. These materials were shown here to become supertough when blended with a maleated SEBS block copolymer elastomer. On the other hand, SEBS-*g*-MA does not effectively toughen MXD6, evidently because MXD6 is not inherently very ductile, nor nylon-6, because the rubber particles formed are too small[3,6]. Nylon-6/MXD6 mixtures prepared under conditions that do not lead to phase homogenization are not effectively toughened by SEBS-*g*-MA for several possible reasons, including the incompatibility of the two polyamides. Thus, the phase-homogenized polyamide mixtures are uniquely useful for producing a toughened material. In our opinion, the keys to this lie in the following. Apparently, the repulsive interaction between nylon-6 and MXD6 segments is weak so that relatively few exchange reactions are needed to achieve melt phase homogeneity, which is important for retention of crystallinity. The nylon-6 units bring to this mixture a relatively higher level of inherent ductility than MXD6 possesses. Addition of MXD6 to nylon-6 changes the rubber phase morphology to give larger particles that are within the optimal range for toughening. This functionalized rubber is too effectively dispersed (or emulsified) in the nylon-6 matrix. Note that nylon-6 is monofunctional in terms of its ability to react with anhydrides, whereas MXD6, like nylon-6,6, is difunctional in this regard. We suggested earlier[4] that this difference in functionality is the cause for these major differences in rubber particle morphology. According to this view, the role of MXD6 in the current system is a chemical one that might also be served by other difunctional polyamides provided phase homogenization can be effected.

ACKNOWLEDGEMENTS

The authors express their appreciation to Mitsubishi Gas Chemical Co. for making this research possible and to the US Army Research Office for their support.

REFERENCES

1 Takeda, Y. and Paul, D. R. *Polymer* 1991, **32**, 2771
2 Ellis, T. S. *Macromolecules* 1989, **22**, 742
3 Oshinski, A. J., Keskkula, H. and Paul, D. R. *Polymer* 1992, **33**, 269
4 Oshinski, A. J., Keskkula, H. and Paul, D. R. *Polymer* 1992, **33**, 284
5 Modic, M. J. and Pettick, L. A. *Plast. Eng.* 1991, **47**, 37
6 Gilmore, D., Kirkpatrick, J. and Modic, M. J. *Soc. Plast. Eng., Tech. Papers, ANTEC* 1990, **36**, 1228
7 Wu, S. *Polymer* 1985, **26**, 1855
8 Wu, S. *Polym. Eng. Sci.* 1987, **27**, 335
9 Borggreve, R. J. M., Gaymans, R. J., Schuijer, J. and Ingen Housz, J. F. *Polymer* 1987, **28**, 1489
10 Borggreve, R. J. M. and Gaymans, R. J. *Polymer* 1989, **30**, 63
11 Gaymans, R. J. and Borggreve, R. J. M. in 'Contemporary Topics in Polymer Science' (Ed. B. M. Culberson), Plenum Press, New York and London, 1989, Vol. 6, p. 461
12 Bucknall, C. B. 'Toughened Plastics', Applied Science, London, 1977
13 Kinloch, A. J. and Young, R. J. (eds.) 'Fracture Behavior of Polymers', Elsevier Applied Science, London and New York, 1990
14 Hobbs, S. Y., Bopp, R. C. and Watkins, V. H. *Polym. Eng. Sci.* 1983, **23**, 380
15 Flexman, E. A. *Polym. Eng. Sci.* 1979, **19**, 564
16 Hobbs, S. Y., Dekkers, M. E. J. and Watkins, V. W. *J. Mater. Sci.* 1989, **24**, 2025
17 Lawson, D., Hergenrother, W. L. and Matlock, M. G. *J. Appl. Polym. Sci.* 1990, **39**, 2331
18 Greco, R., Malinconico, M., Martuscelli, E., Ragosta, G. and Scarinizi, G. *Polymer* 1987, **28**, 1185
19 Greco, R., Malinconico, M., Martuscelli, E., Ragosta, G. and Scarinizi, G. *Polymer* 1988, **29**, 1418
20 Chuang, H. and Han, C. D. *J. Appl. Polym. Sci.* 1985, **30**, 165
21 Cimmino, S., D'Orazio, L., Greco, R., Maglio, G., Malinconico, M., Mancarella, C., Martuscelli, E., Palumbo, R. and Ragosta, G. *Polym. Eng. Sci.* 1984, **24**, 48
22 MacKnight, W. J., Lenz, R. W., Musto, P. V. and Somani, R. J. *Polym. Eng. Sci.* 1985, **25**, 1124
23 Ide, F. and Hasegawa, A. *J. Appl. Polym. Sci.* 1974, **18**, 963
24 Ong, E. S., Kim, Y. and Williams, H. L. *J. Appl. Polym. Sci.* 1986, **31**, 367
25 Paul, D. R. and Altamirano, J. O. *Adv. Chem. Ser.* 1975, **142**, 371
26 Ando, Y. and Yoon, D. Y. *ACS Polym. Prepr.* 1987, **28**, 26
27 Hahn, B. R., Wendorff, J. H. and Yoon, D. Y. *Macromolecules* 1985, **18**, 718
28 Myers, M. E., Wims, A. M., Ellis, T. S. and Barnes, J. *Macromolecules* 1990, **23**, 2807
29 Wada, Y. and Kasahara, T. *J. Appl. Polym. Sci.* 1967, **11**, 1661
30 Schooten, J., Hoorn, H. and Boerma, J. *Polymer* 1961, **2**, 161
31 Robeson, L. M. and Faucher, J. A. *J. Polym. Sci., Polym. Lett.* 1969, **7**, 35
32 Cheng, T. W., Keskkula, H. and Paul, D. R. *Polymer* in press
33 Oostenbrink, A. J., Molenaar, L. J. and Gaymans, R. J. Poster given at 6th Annual Meeting of the Polymer Processing Society, Nice, France, 18–20 April, 1990
34 Kim, H., Keskkula, H. and Paul, D. R. *Polymer* 1991, **32**, 1447
35 Keskkula, H., Turley, S. G. and Boyer, R. F. *J. Appl. Polym. Sci.* 1971, **15**, 351
36 Wagner, E. R. and Robeson, L. M. *Rubber Cham. Technol.* 1970, **43**, 1129